Appl Microbiol Biotechnol (2013) 97:1669–1678
DOI 10.1007/s00253-012-4298-3

Implementation of a transhydrogenase-like shunt to counter redox imbalance during xylose fermentation in *Saccharomyces cerevisiae*

Hiroyuki Suga · Fumio Matsuda · Tomohisa Hasunuma · Jun Ishii · Akihiko Kondo

Received: 28 March 2012 / Revised: 10 July 2012 / Accepted: 11 July 2012 / Published online: 1 August 2012

Abstract Three enzymes responsible for the transhydrogenase-like shunt, including malic enzyme (encoded by *MAE1*), malate dehydrogenase (*MDH2*), and pyruvate carboxylase (*PYC2*), were overexpressed to regulate the redox state in xylose-fermenting recombinant *Saccharomyces cerevisiae*. The YPH499XU/MAE1 strain was constructed by overexpressing native Mae1p in the YPH499XU strain expressing xylose reductase and xylitol dehydrogenase from *Scheffersomyces stipitis*, and native xylulokinase. Analysis of the xylose fermentation profile under semi-anaerobic conditions revealed that the ethanol yield in the YPH499XU/MAE1 strain (0.38±0.01 g g^{-1} xylose consumed) was improved from that of the control strain (0.31±0.01 g g^{-1} xylose consumed). Reduced xylitol production was also observed in YPH499XU/MAE1, suggesting that the redox balance was altered by Mae1p overexpression. Analysis of intracellular metabolites showed that the redox imbalance during xylose fermentation was partly relieved in the transformant. The specific ethanol production rate in the YPH499XU/MAE1–MDH2 strain was 1.25-fold higher than that of YPH499XU/MAE1 due to the additional overexpression of Mdh2p, whereas the ethanol yield was identical to that of YPH499XU/MAE1. The specific xylose consumption rate was drastically increased in the YPH499XU/MAE1–MDH2–PYC2 strain. However, poor ethanol yield as well as increased production of xylitol was observed. These results demonstrate that the transhydrogenase function implemented in *S. cerevisiae* can regulate the redox state of yeast cells.

Keywords Transhydrogenase-like shunt · Malic enzyme · Anaplerotic pathway · Xylose fermentation · *Saccharomyces cerevisiae*

H. Suga · A. Kondo (✉)
Department of Chemical Science and Engineering,
Graduate School of Engineering, Kobe University,
1-1 Rokkodaicho, Nada-ku,
Kobe, Hyogo 657-8501, Japan
e-mail: akondo@kobe-u.ac.jp

F. Matsuda · T. Hasunuma · J. Ishii
Organization of Advanced Science and Technology,
Kobe University,
1-1 Rokkodaicho, Nada-ku,
Kobe, Hyogo 657-8501, Japan

F. Matsuda · A. Kondo
RIKEN Biomass Engineering Program,
1-7-22 Suehirocho, Tsurumi,
Yokohama 230-0045, Japan

Introduction

Improvements in xylose fermentation have been extensively studied by manipulating the initial xylose assimilation pathway because xylose is the dominant pentose sugar in the hydrolysates of lignocellulosic biomass (Hahn-Hagerdal et al. 2007; Matsushika et al. 2009; Nevoigt 2008; Van Vleet and Jeffries 2009). Anaerobic xylose fermentation by *Saccharomyces cerevisiae* was first demonstrated by heterologous expression of the *XYL1* (Rizzi et al. 1988) and *XYL2* (Rizzi et al. 1989) genes encoding xylose reductase (XR) and xylitol dehydrogenase (XDH) from *Scheffersomyces* (*Pichia*) *stipitis*, respectively (Kötter and Ciriacy 1993; Tantirungkij et al. 1993) (Fig. 1). However, the recombinant strains consumed xylose at a slower rate and exhibited significant byproduct (xylitol) formation (Eliasson et al. 2000; Ho et al. 1998; Johansson and Hahn-Hagerdal 2002;

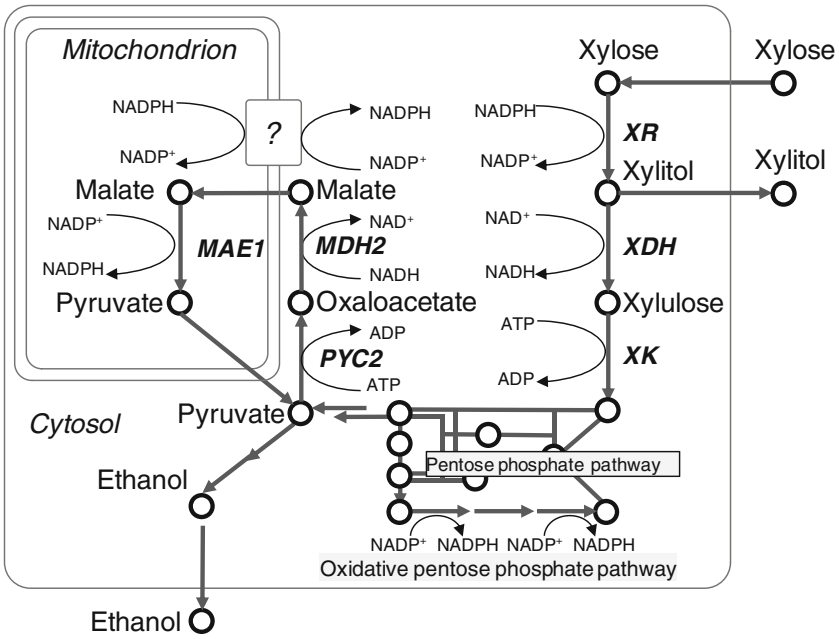

Fig. 1 Biochemical reactions related to the transhydrogenase-like shunt and xylose assimilation. The intracellular localization of each reaction is shown. The mitochondrial redox shuttle for NADPH transport has not been identified. The details of the pentose phosphate pathway are not shown. *XR* xylose reductase, *XDH* xylitol dehydrogenase, *XK* xylulokinase

Katahira et al. 2008; Sonderegger and Sauer 2003; Verho et al. 2003; Watanabe et al. 2007). One reason for the result is a difference in the coenzyme usage of *S. stipitis* XR and XDH, which preferentially use NADPH and NAD^+, respectively (Fig. 1). The redox imbalance should hamper the conversion of xylose to xylulose by XR and XDH (Bruinenberg et al. 1983; Jeffries and Jin 2004). In order to improve the redox imbalance, a series of metabolic engineering studies were conducted by protein engineering to alter cofactor usage (Bro et al. 2006; Klimacek et al. 2010; Matsushika et al. 2008; Verho et al. 2003; Watanabe et al. 2007). Additionally, changing the intracellular redox balance in xylose-fermenting *S. cerevisiae* has also been attempted by implementing additional metabolic reactions. The imbalance could be relieved by the activity of pyridine nucleotide transhydrogenase catalyzing the following reaction: $NADH+NADP^+ \rightarrow NAD^+ + NADPH$ (Arkblad et al. 1996; Sauer et al. 2004). Although pyridine nucleotide transhydrogenase plays an important role in regulating the cellular redox state in many organisms, *S. cerevisiae* does not possess a gene encoding this enzyme (Anderlund et al. 1999). Furthermore, it has been demonstrated that heterologous expression of a bacterial transhydrogenase in *S. cerevisiae* resulted in increased production of glycerol rather than ethanol (Nissen et al. 2001).

In this study, an alternative transhydrogenase function was implemented to *S. cerevisiae* by an activation of metabolic shunt consists of pyruvate carboxylase (PYC), malate dehydrogenase (MDH), and malic enzyme (MAE). It has been suggested that the metabolic shunt involving anaplerotic reactions may function in a fashion similar to that of transhydrogenase (Fig. 1) (Blombach et al. 2011; Moreira dos Santos et al. 2004). Through this shunt, pyruvate is sequentially converted to oxaloacetate, malate, and pyruvate by the activities of PYC (catalyzing the following reaction: $pyruvate+ATP \rightarrow oxaloacetate+ADP+Pi+CO_2$), MDH ($oxaloacetate+NADH \rightarrow malate+NAD^+$), and MAE ($malate+NADP^+ \rightarrow pyruvate+NADPH+CO_2$) as shown in Fig. 1. As the coenzyme preferences of MDH and MAE in *S. cerevisiae* are NADH and $NADP^+$, respectively (Boles et al. 1998), the net stoichiometry of the shunt is: $ATP+NADH+NADP^+ \rightarrow ADP+Pi+NAD^+ + NADPH$, indicating that a transhydrogenase-like function can be implemented at the expense of ATP. In this study, the metabolic shunt was activated by overexpressing the Mae1p, Mdh2p, and Pyc2p proteins to implement the transhydrogenation function in xylose-fermenting yeast expressing XR, XDH, and XK.

Materials and methods

Yeast strains, plasmids, and transformation

The yeast strains and plasmids used in this study are listed in Table 1. The growth conditions and DNA techniques used have been previously described (Katahira et al. 2006). The *MDH2, MAE1,* and *PYC2* genes were amplified using the genomic DNA of the *S. cerevisiae* strain BY4741 (Brachmann et al. 1998; Ishii et al. 2009) as a template with the primer sets 5′-CCGGTCGACATGCCTCACTCAGTTACACCATCC-3′/5′-CGGCCCGGGTTAAGATGATGCAGATCTCGATGC-3′, 5′-CCGGTCGACATGCTTAGAACCAGACTATCCGTT-3′/5′-CCGGAATTCCTACAATTGGTTGGTGTGCACCGA-3′, and 5′-GCCGTCGACATGAGCAGTAGCAAGAAATTGG-3′/5′-GGCCCCGGGTTACTTTTTTTGGGATGGGGGTAGGG-3′,

Table 1 Yeast strains and plasmids used in this study

Strain or plasmid	Description	Source or reference
Strains		
Saccharomyces cerevisiae YPH499	*MAT***a** *ade2 his3 leu2 lys2 trp1 ura3*	Purchased from Stratagene (LaJolla, CA)
S. cerevisiae YPH499XU	*S. cerevisiae* YPH499 (pIUX1X2XK)	Hasunuma et al. (2011)
YPH499XU/MAE1	YPH499XU (pGK404ScMAE1)	Current study
YPH499XU/MAE1–PYC2	YPH499XU (pGK404ScMAE1, pGK405ScPYC2)	Current study
YPH499XU/MAE1–MDH2	YPH499XU (pGK404ScMAE1, pGK402ScMDH2)	Current study
YPH499XU/MAE1–MDH2–PYC2	YPH499XU (pGK404ScMAE1, pGK402ScMDH2, pGK405ScPYC2)	Current study
YPH499XU/pGK404	YPH499XU (pGK404)	Current study
YPH499XU/pGK404–pGK402	YPH499XU (pGK404, pGK402)	Current study
YPH499XU/pGK404–pGK405	YPH499XU (pGK404, pGK405)	Current study
YPH499XU/pGK404–pGK402–pGK405	YPH499XU (pGK404, pGK402, pGK405)	Current study
Plasmids		
pIUX1X2XK	*URA3*, intracellular co-expression of *XYL1* (xylose reductase from *Scheffersomyces stipitis)*, *XYL2* (xylitol dehydratase from *S. stipitis)*, and *XYS1* (xylulokinase from *S. cerevisiae)* genes.	Katahira et al. (2006)
pGK402ScMDH2	*ADE2,* expression of *S. cerevisiae MDH2* gene under the control of the *PGK1* promoter	Current study
pGK404ScMAE1	*TRP1,* expression of *S. cerevisiae MAE1* gene under the control of the *PGK1* promoter	Current study
pGK405ScPYC2	*LEU2,* expression of *S. cerevisiae PYC2* gene under the control of the *PGK1* promoter	Current study
pGK402	*ADE2,* no insert (control plasmid)	Ishii et al. (2009)
pGK404	*TRP1,* no insert (control plasmid)	Ishii et al. (2009)
pGK405	*LEU2,* no insert (control plasmid)	Ishii et al. (2009)

respectively. The amplified fragments were digested and ligated into the pCR-Blunt II-TOPO vector (Invitrogen, Carlsbad, CA) to yield the pCR-Blunt II-TOPO-*MDH2,* pCR-Blunt II-TOPO-*MAE1,* and pCR-Blunt II-TOPO-*PYC2* plasmids, respectively. The purified plasmids were used for sequence confirmation. Plasmids containing the *MDH2*, *MAE1,* and *PYC2* coding regions were digested and ligated into the *Sal*I–*Xma*I, *Sal*I–*Eco*RI, and *Sal*I–*Xma*I sites of the pGK402, pGK404, and pGK405 plasmids (Ishii et al. 2009) to yield the pGK402ScMDH2, pGK404ScMAE1, and pGK405ScPYC2 plasmids, respectively.

Transformations were performed using the lithium-acetate method as previously described (Ito et al. 1983; Katahira et al. 2006). The pGK402ScMDH2, pGK404ScMAE1, and pGK405ScPYC2 plasmids were digested with *Eco*RV, *Bsp*EI, and *Afl*II, respectively. The linear products were transformed into the *S. cerevisiae* strain YPH499XU (Hasunuma et al. 2011).

Xylose and glucose fermentations

The yeast transformants were aerobically cultivated in yeast extract peptone dextrose (YPD) medium (10 g l^{-1} yeast extract, 20 g l^{-1} peptone, and 20 g l^{-1} D-glucose) for 48 h at 30 °C. The cells were collected by centrifugation at 1,000×*g* for 5 min at 4 °C and washed twice with sterile water. The cells were then inoculated into 50 ml of fermentation medium. For xylose fermentation, YPX medium containing 10 g l^{-1} yeast extract, 20 g l^{-1} peptone, and 50 g l^{-1} xylose was used. Medium containing 10 g l^{-1} yeast extract, 20 g l^{-1} peptone, and 50 g l^{-1} glucose was used for glucose fermentation. All fermentations were performed at 30 °C with mild agitation in 100-ml closed bottles equipped with a bubbling CO_2 outlet. The initial cell concentration was adjusted to 50 g of wet cells l^{-1} (corresponding to OD 33.3 and 11 g of dry cells l^{-1}). The wet cell weight was determined by weighing the cell pellet that was harvested by centrifugation at 1,000×*g* for 5 min. To determine the concentrations of ethanol, glucose, glycerol, xylitol, and xylose in the fermentation medium, the supernatant obtained by centrifugation at 14,000×*g* at 4 °C for 5 min was applied to a high-performance liquid chromatography (HPLC) system (Shimadzu, Kyoto, Japan) equipped with a Shim-pack SPR-Pb column (7.8× 250 mm; Shimadzu) and an RID-10A refractive index detector (Shimadzu). The HPLC system was operated at 80 °C with water at a flow rate of 0.6 ml min^{-1} as the mobile phase.

Metabolite analysis

Targeted analysis of malate and nicotinamide adenine dinucleotides in *S. cerevisiae* cells was performed using the following procedure. The cold methanol method was used to collect YPH499XU/MAE1 and YPH499XU/pGK404 cells (Spura et al. 2009). Three milliliters of cell suspension was transferred to 6 ml of precooled 60 % (v/v) methanol solution at −50 °C and mixed quickly by inversion. Samples were centrifuged at 10,000×*g* at −9 °C for 5 min and frozen in liquid nitrogen after decanting. The other strains were analyzed using the filtration method. Both methods produced essentially the same results for the target metabolites (Kato et al. 2012). Fermentation liquid (3 ml) was filtered through a membrane filter (Omnipore, 0.45-μm, 25-mm diameter polytetrafluoroethylene; Millipore, MA). Immediately after filtration, the yeast cells were washed with 5 ml of cold aqueous ammonium hydrogen carbonate (50 mM, at 4 °C), transferred into an Eppendorf tube with a membrane filter, and frozen in liquid nitrogen. The time required for the procedure was approximately 45 s. The samples were stored at −80 °C until analysis. Metabolites were extracted from the cells by adding 1.5 ml of methanol containing an internal standard (32.3 nM (+)-10-camphorsulfonic acid) and shaking the samples with a zirconia bead (5.0 mm) for 10 min at 1,500 rpm (Shake Master Neo; Biomedical Science, Japan). Following centrifugation at 4 °C for 5 min at 15,000×*g*, 400 μl of chloroform and 160 μl of MilliQ water were added to 500 μl of the supernatant. After mixing and centrifugation at 4 °C for 5 min at 15,000×*g*, the water phase of the extract (300 μl) was dried under vacuum and dissolved in 50 μl of MilliQ water. The extracts were analyzed using a liquid chromatography-triple quadrupole mass spectrometry (LC-QqQ-MS) system (LC: Agilent 1200 series; MS, Agilent 6460 with Jet Stream Technology; Agilent Technologies, Waldbronn, Germany) controlled by MassHunter Workstation Data Acquisition software v. B. 04.01 (Agilent Technologies). The LC-QqQ-MS analysis was performed under the following conditions: column, Unison UK-C18 column (2.0×150 mm, particle size of 3 μm; Imtakt Corp., Kyoto, Japan); mobile phase, 10 mM tributylamine/15 mM acetic acid in water (A) and methanol (B); flow rate, 0.3 ml min^{-1}; gradient curve, 0 % B at 0 min, 0 % B at 8 min, 90 % B at 24 min, 0 % B at 24.1 min, and 0 % B at 30 min; injection volume, 3 μl; column temperature, 35 °C; mode of mass analysis, multiple reactions monitoring (MRM) at negative ion mode. The detailed MRM and ionization conditions for the analysis were previously reported (Kato et al. 2012). The peak of a target metabolite was identified by comparing its chromatographic behavior with that of an authentic standard, and its peak area was determined using the MassHunter Quantitative Analysis v. B. 04.00 software (Agilent Technologies). Normalized peak areas (relative to that of internal standard) are used to represent the relative abundances of metabolites in the samples. Ratios of NADH/NAD^+ and NADPH/$NADP^+$ were determined by using the normalized peak area.

Results

Role of mitochondrial malic enzyme in xylose fermentation

The functionality of the metabolic shunt in *S. cerevisiae* has been doubted because MAE is specifically expressed in the mitochondria (Boles et al. 1998), whereas PYC is active in the cytosol (Fig. 1) (Bakker et al. 2001). To investigate the role of mitochondrial MAE in xylose fermentation, a recombinant strain (YPH499XU/MAE1) was constructed by homologous overexpression of Mae1p in the xylose-fermenting recombinant strain YPH499XU, which harbors three genes for xylose assimilation: XK from *S. cerevisiae*, and XR and XDH from *S. stipitis* (Table 1). The performance of YPH499XU/MAE1 was compared with that of its vector control (YPH499XU/pGK404) in batch fermentation under semi-anaerobic conditions using YPX medium containing yeast extract, peptone, and xylose (Fig. 2a–c and Table 2). The fermentation data revealed that the ethanol yield in YPH499XU/MAE1 (0.38±0.01 g g^{-1} xylose consumed) was higher than that of the vector control (0.31±0.01 g g^{-1} xylose consumed) (Fig. 2b and Table 2), because the xylitol yield of YPH499XU/MAE1 (0.19±0.01 g g^{-1} xylose consumed) was lower than that of the vector control (0.28±0.02 g g^{-1} xylose consumed) (Fig. 2c and Table 2). The specific xylose consumption rate of YPH499XU/MAE1 was also 28 % higher than that of YPH499XU/pGK404 (Fig. 2a and Table 2). These results suggest that the redox balance in the YPH499XU/MAE1 strain was altered by the up-regulation of Mae1p expression.

To further confirm the role of Mae1p, the levels of malate and nicotinamide adenine dinucleotides in yeast cells were analyzed using LC-QqQ-MS. Because an increased ethanol yield was observed in batch fermentation using YPX medium, the intracellular metabolites were extracted from the yeast cells fermented under identical conditions (Fig. 2d–f). Comparison of the metabolite levels in YPH499XU/MAE1 with that of the vector control (YPH499XU/pGK404) revealed that Mae1p overexpression decreased the levels of malate in the yeast cells (Fig. 2d). Furthermore, the NADPH/$NADP^+$ ratio was slightly increased in the YPH499XU/MAE1 strain (Fig. 2e), indicating that the regeneration of NADPH was increased by the activation of a metabolic reaction catalyzed by MAE (Fig. 1). Furthermore, the production of malate from oxaloacetate may be activated

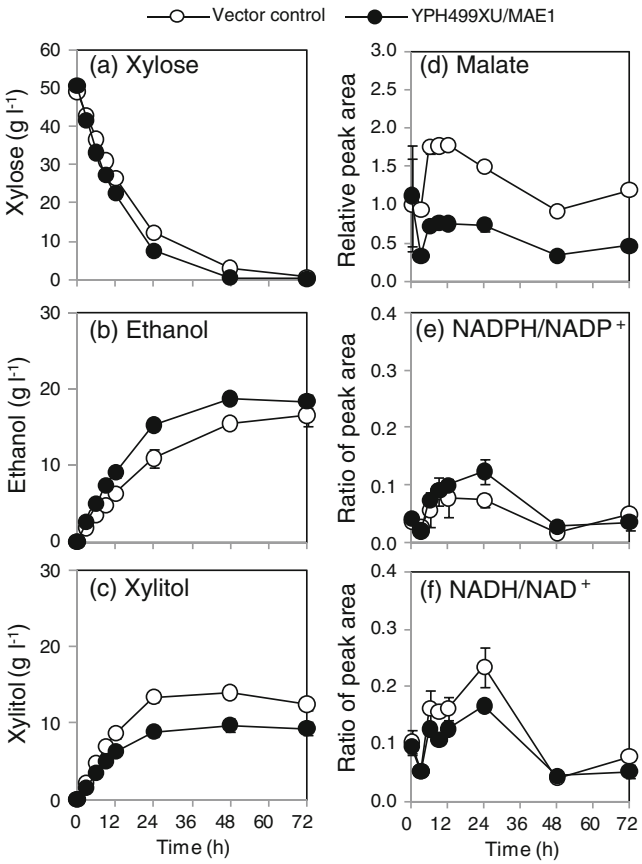

Fig. 2 Fermentation and intracellular metabolite profiles of the recombinant *Saccharomyces cerevisiae* strain YPH499XU/MAE1 cultured in 50 g l^{-1} xylose. Concentrations of xylose (**a**), ethanol (**b**), and xylitol (**c**) in the culture medium were determined using HPLC. Relative levels of malate (**d**), NADPH/$NADP^+$ ratio (**e**), and NADH/NAD^+ ratio (**f**) were determined using LC-QqQ-MS. Data derived from YPH499XU/MAE1 (*filled circle*) and its vector control (YPH499XU/pGK404; *open circle*) are shown. Signal intensity (peak area) are used to represent relative abundances of intracellular metabolites. Each data point represents the mean (SD) values obtained from three replicate fermentations

in the YPH499XU/MAE1 strain because the NADH/NAD^+ ratio was slightly decreased (Fig. 2f).

Distinct effects of additional overexpression of Pyc2p and Mdh2p

For further activation of the metabolic shunt, two recombinant strains YPH499XU/MAE1–PYC2 and YPH499XU/MAE1–MDH2 were constructed by introducing the native *PYC2* and *MDH2* genes, respectively (Table 1). YPH499XU/MAE1–PYC2 showed rather poor performance in xylose fermentation as shown in Table 2. In the case of the YPH499XU/MAE1–MDH2 strain, the yields of ethanol (0.39±0.003 g g^{-1} xylose consumed) and xylitol (0.20±0.003 g g^{-1} xylose consumed) were essentially identical to that of YPH499XU/MAE1 (0.38±0.01 and 0.19±0.01 g g^{-1} xylose consumed, respectively) (Fig. 3 and Table 2). On the other hand, the rates of specific xylose consumption (0.29±0.01 g g dry $cells^{-1}$ h^{-1}) and ethanol production (0.09±0.001 g g dry $cells^{-1}$ h^{-1}) were 24 % and 25 % higher than that of YPH499XU/MAE1, and also 41 % and 40 % higher than that of the vector control (YPH499XU/pGK404–pGK402), respectively (Fig. 3 and Table 2). The levels of malate and nicotinamide adenine dinucleotides (Fig. 3d–f) were altered during fermentation in a manner similar to that of YPH499XU/MAE1 (Fig. 2d–f). However, the malate levels and the NADPH/$NADP^+$ ratio in the YPH499XU/MAE1–MDH2 strain (Fig. 3d and e) tended to be higher than those of the YPH499XU/MAE1 strain (Fig. 2d and e).

Simultaneous overexpression of Mae1p, Mdh2p, and Pyc2p

Effects of simultaneous overexpression of Mae1p, Mdh2p, and Pyc2p on xylose fermentation were investigated. The specific xylose consumption rate of the YPH499XU/MAE1–MDH2–PYC2 strain increased to 0.40±0.003 g g dry $cells^{-1}$ h^{-1}, which was 81 % higher than that of the vector control (Fig. 4a and Table 2). To investigate the metabolic events occurring in the YPH499XU/MAE1–MDH2–PYC2 strain, the levels of intermediates were analyzed by LC-QqQ-MS (Fig. 4d–f). The levels of malate were similar to that observed with the vector control, indicating that a sufficient amount of malate was produced by the overexpressed Pyc2p and Mdh2p enzymes (Fig. 4d). In addition, the NADPH/$NADP^+$ levels were significantly increased in the YPH499XU/MAE1–MDH2–PYC2 strain (Fig. 4e). The metabolic states should preferable to increase the turnover of the XR reaction and xylose uptake. Despite the faster xylose consumption, poor ethanol yield was obtained from the YPH499XU/MAE1–MDH2–PYC2 strains because xylitol production was drastically increased (Fig. 4b and c). Metabolite analysis also demonstrated that the NADH/NAD^+ ratio was increased in the strain (Fig. 4f). The high NADH/NAD^+ ratio would disturb the reaction catalyzed by XDH, thereby leading to the secretion of excess xylitol into the medium.

Furthermore, YPH499XU/MAE1–MDH2–PYC2 showed a diauxic xylose conversion pattern because it began to consume xylitol after the depletion of xylose (Fig. 4a and c). Due to the xylitol assimilation capability, the ethanol concentration in the medium gradually increased until 72 h after the initiation of fermentation. Although the specific ethanol production rate during 24 to 48 h after fermentation initiation was very slow (4.7±0.3 mg g dry $cells^{-1}$ h^{-1}), the ethanol yield from xylitol (0.33±0.02 g g^{-1} xylose consumed) was comparable to that from xylose. It has been reported that other yeasts, such as *Candida utilis* and *Rhodotorula toruloides* can utilize xylitol (Hsiao et al. 1982). These results suggest that the transhydrogenase-like

Table 2 Efficiencies of recombinant yeast strains cultured in 50 g l^{-1} xylose[a]

Strains	Xylose consumption rate (g l^{-1} h^{-1}) and specific xylose consumption rate (g g dry cells^{-1} h^{-1})[b]	Ethanol production rate (g l^{-1} h^{-1}) and specific ethanol production rate (g g dry cells^{-1} h^{-1})[b]	Yield (g g^{-1} xylose consumed)		
			Ethanol	Glycerol	Xylitol
YPH499XU/MAE1	2.60±0.05 (0.23±0.01)	0.82±0.05 (0.08±0.01)	0.38±0.01	0.02±0.004	0.19±0.01
YPH499XU/MAE1–PYC2	1.16±0.09 (0.11±0.01)	0.33±0.03 (0.03±0.003)	0.29±0.01	0.02±0.003	0.20±0.004
YPH499XU/MAE1–MDH2	3.22±0.07 (0.29±0.01)	1.03±0.01 (0.09±0.001)	0.39±0.003	0.03±0.003	0.20±0.003
YPH499XU/MAE1–MDH2–PYC2	4.37±0.03 (0.40±0.003)	1.16±0.02 (0.11±0.002)	0.27±0.003	0.06±0.004	0.42±0.01
YPH499XU/pGK404	2.03±0.06 (0.20±0.01)	0.53±0.01 (0.05±0.001)	0.31±0.01	0.01±0.002	0.28±0.02
YPH499XU/pGK404–pGK405	2.15±0.05 (0.20±0.01)	0.57±0.02 (0.05±0.002)	0.32±0.01	0.01±0.001	0.28±0.01
YPH499XU/pGK404–pGK402	2.28±0.14 (0.21±0.01)	0.73±0.02 (0.07±0.002)	0.33±0.01	0.01±0.002	0.30±0.004
YPH499XU/pGK404–pGK402–pGK405	2.41±0.05 (0.22±0.01)	0.68±0.03 (0.06±0.003)	0.31±0.02	0.01±0.002	0.27±0.01

[a] Each data point represents the mean ± SD obtained from three replicate fermentations

[b] Specific xylose consumption rate and specific ethanol production rate are shown in brackets

shunt may have a role in the carbon assimilation function in these yeasts.

Effects of the transhydrogenase-like shunt on glucose fermentation

As mentioned above, the transhydrogenase-like function of the shunt requires the expenditure of ATP. Since ATP is essential for various cellular processes including the glucose assimilation pathway, the additional consumption of ATP by the overexpression of Mae1p, Mdh2p, and Pyc2p is likely to affect the efficiency of glucose fermentation. The aerobic growth of all the strains in YPD medium was essentially the same as that of the control strains (data not shown). The glucose fermentation profiles of the YPH499XU/MAE1 and YPH499XU/MAE1–MDH2 strains were essentially identical to those of the vector controls (YPH499XU/pGK404 and YPH499XU/pGK404–pGK402, respectively), as shown in Table 3. On the other hand, the specific glucose consumption rate of the YPH499XU/MAE1–MDH2–PYC2 strain (2.15±0.10 g g dry cells^{-1} h^{-1}) was 45 % higher than that of the vector control (1.48±0.13 g g dry cells^{-1} h^{-1}) (Table 3). The higher specific glucose consumption rate may be attributed to the substrate specificity of MAE encoded by *MAE1* (Boles et al. 1998). It has been demonstrated that, in addition to $NADP^+$, Mae1p enzyme could use NAD^+ as an electron acceptor. When NAD^+ is used as an electron acceptor by MAE, the shunt would drain ATP without performing the transhydrogenase function. In order to produce more ATP, the YPH499XU/MAE1–MDH2–PYC2 strain would increase its glucose uptake rate.

Discussion

In this study, three enzymes responsible for the transhydrogenase-like shunt including Mae1p, Mdh2p, and Pyc2p were overexpressed to regulate the redox state in the xylose-fermenting recombinant *S. cerevisiae*. As mentioned in the Introduction section, although the heterologous expression of XR and XDH from *S. stipitis* enabled anaerobic xylose fermentation, the ethanol yield and the specific xylose consumption rate were lower than that of glucose fermentation (Kötter and Ciriacy 1993; Tantirungkij et al. 1993). It has been suggested that the poor performance may be due to an intracellular redox imbalance caused by the difference in coenzyme preference between *S. stipitis* XR and XDH during xylose fermentation. Since XR and XDH preferentially use NADPH and NAD^+, respectively, the excess $NADP^+$ and NADH formed would hamper the progress of the xylose assimilation reactions.

Metabolic flux analyses of the xylose-fermenting recombinant strains revealed that the amount of NADPH required for the XR reaction was regenerated from $NADP^+$ by the oxidative pentose phosphate pathway (Fig. 1) (Grotkjaer et al. 2005; Krahulec et al. 2010; Pitkanen et al. 2003; Sonderegger et al. 2004). The significant production of xylitol also indicated that a mechanism for the regeneration

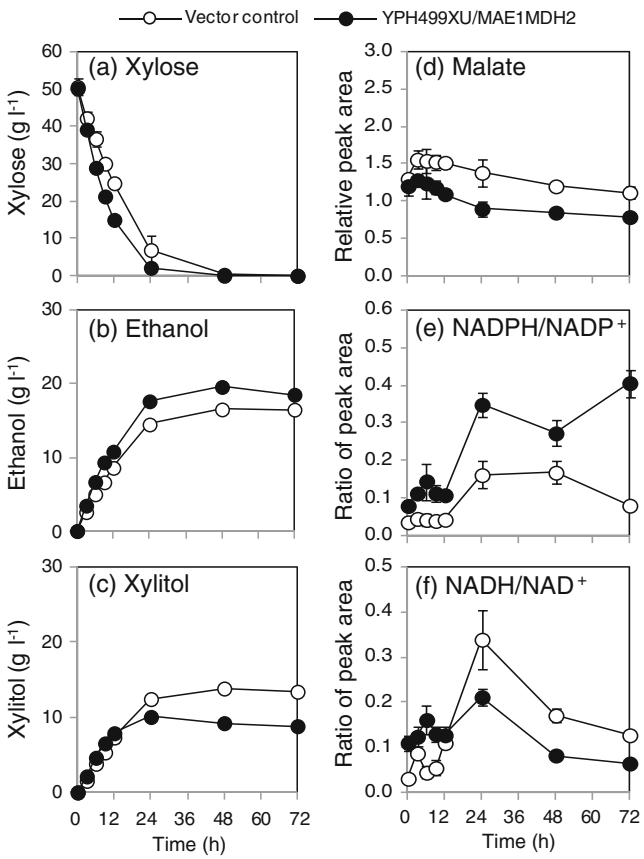

Fig. 3 Fermentation and intracellular metabolite profiles of the recombinant *S. cerevisiae* strain YPH499XU/MAE1–MDH2 cultured in 50 g l^{-1} xylose. Concentrations of xylose (**a**), ethanol (**b**), and xylitol (**c**) in the culture medium were determined using HPLC. Malate concentration (**d**), NADPH/$NADP^+$ ratio (**e**), and NADH/NAD^+ ratio (**f**) were determined using LC-QqQ-MS. Data obtained from YPH499XU/MAE1–MDH2 (*filled circle*) and its vector control (YPH499XU/pGK404–pGK402; *open circle*) are shown. Signal intensity (peak area) are used to represent relative abundances of intracellular metabolites. Each data point represents the mean (SD) values obtained from three replicate fermentations

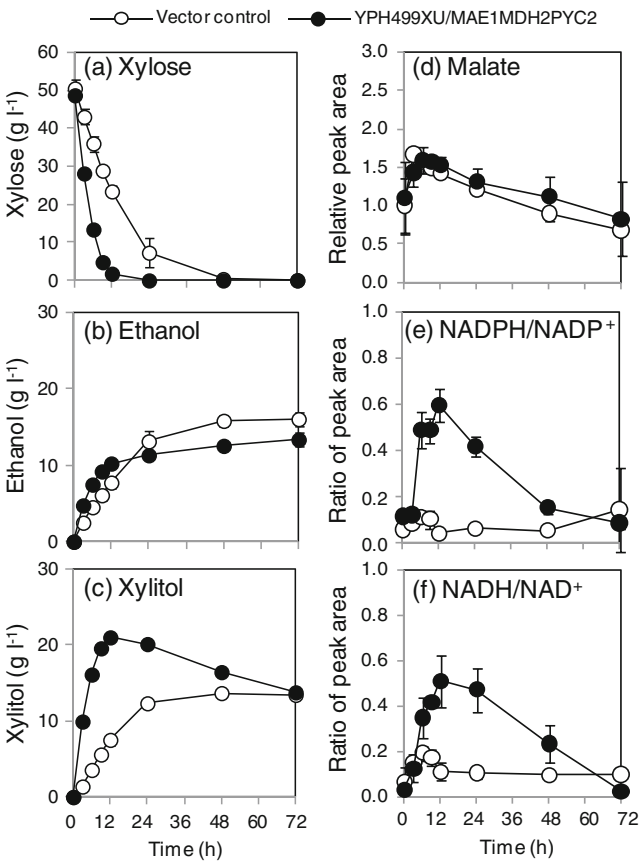

Fig. 4 Fermentation and intracellular metabolite profiles of the recombinant *S. cerevisiae* strain YPH499XU/MAE1–MDH2–PYC2 cultured in 50 g l^{-1} xylose. Concentrations of xylose (**a**), ethanol (**b**), and xylitol (**c**) in the culture medium were determined using HPLC. Malate concentration (**d**), NADPH/$NADP^+$ ratio (**e**), and NADH/NAD^+ ratio (**f**) were determined using LC-QqQ-MS. Data derived from YPH499XU/MAE1–MDH2–PYC2 (*filled circle*) and its vector control (YPH499XU/pGK404–pGK402–pGK405; *open circle*) are shown. Signal intensity (peak area) are used to represent relative abundances of metabolites in the yeast cells. Each data point represents the mean (SD) values obtained from three replicate fermentations

of NAD^+ from NADH might also be activated for more efficient xylose fermentation (Fig. 1). In many microorganisms other than *S. cerevisiae*, it has been demonstrated that the redox imbalance can be relieved by the activity of pyridine nucleotide transhydrogenase (Arkblad et al. 1996; Sauer et al. 2004). However, the heterologous expression of a bacterial transhydrogenase in xylose-fermenting *S. cerevisiae* did not improve ethanol yields (Nissen et al. 2001). Therefore, the application of a transhydrogenase-like shunt involving anaplerotic reactions was investigated in this study (Blombach et al. 2011; Moreira dos Santos et al. 2004).

Although *S. cerevisiae* has three genes for the metabolic shunt, including *MAE1*, *MDH2*, and *PYC2* (Moreira dos Santos et al. 2004), its transhydrogenase-like functionality has been questioned due to the specific expression of Mae1p in mitochondria (Fig. 1) (Bakker et al. 2001). In this regard, previous studies suggested a role for the mitochondrial MAE in regulating the redox balance in the cytosol (Moreira dos Santos et al. 2004). For instance, recombinant *S. cerevisiae* strains overproducing Mae1p and Pyc2p have been previously constructed. While the characteristics of glucose fermentation were generally not affected, a net transhydrogenase effect caused by the metabolic shunts was indirectly supposed from the decreased pentose phosphate pathway flux (Moreira dos Santos et al. 2004). A role for the mitochondrial MAE in xylose fermentation has also been suggested by the analysis of a mutant strain capable of growth on xylose under strictly anaerobic conditions (Sonderegger et al. 2004). The transcriptome analysis revealed that the expression of the *MAE1* gene encoding the mitochondrial MAE was constitutively up-regulated in

Table 3 Efficiencies of recombinant yeast strains cultured in 50 g l^{-1} glucose[a]

Strains	Glucose consumption rate (g l^{-1} h^{-1}) and specific glucose consumption rate (g g dry cells^{-1} h^{-1})[b]	Ethanol production rate (g l^{-1} h^{-1}) and specific ethanol production rate (g g dry cells $^{-1}$ h^{-1})[b]	Yield (g g^{-1} glucose consumed)	
			Ethanol	Glycerol
YPH499XU/MAE1	10.2±0.6 (0.93±0.05)	4.4±0.1 (0.40±0.01)	0.45±0.03	0.06±0.01
YPH499XU/MAE1–MDH2	14.2±0.4 (1.29±0.03)	6.4±0.2 (0.58±0.02)	0.45±0.01	0.06±0.01
YPH499XU/MAE1–MDH2–PYC2	23.6±1.1 (2.15±0.10)	10.5±0.2 (0.96±0.02)	0.44±0.02	0.04±0.01
YPH499XU/pGK404	10.4±0.4 (0.95±0.04)	4.4±0.1 (0.40±0.01)	0.45±0.01	0.06±0.01
YPH499XU/pGK404–pGK402	13.5±0.4 (1.23±0.03)	6.1±0.2 (0.56±0.02)	0.46±0.01	0.05±0.01
YPH499XU/pGK404–pGK402–pGK405	16.3±1.4 (1.48±0.13)	7.2±0.3 (0.66±0.03)	0.46±0.02	0.05±0.01

[a] Each data point represents the mean ± SD values obtained from three replicate fermentations

[b] Specific glucose consumption rate and specific ethanol production rate are shown in brackets

the mutant strain generated by evolutionary engineering of a xylose-fermenting recombinant strain (Sonderegger et al. 2004).

To confirm the role of mitochondrial MAE in xylose fermentation, a recombinant *S. cerevisiae* strain was constructed by overexpressing Mae1p (Table 1). The xylose fermentation data demonstrated that the YPH499XU/MAE1 strain exhibited reduced xylitol production and a consequent increase in ethanol yield (Fig. 2b,c and Table 2). The up-regulation of the MAE reaction by Mae1p overexpression was supported by the analyses of intracellular metabolites, which revealed lower malate levels and higher NADPH/NAD^+ ratio in the YPH499XU/MAE1 strain (Fig. 2d and e). The higher NADPH/NAD^+ ratio indicated that Mae1p enzyme used $NADP^+$ as an electron acceptor in *S. cerevisiae* cells while Mae1p enzyme could also utilize NAD^+ (Boles et al. 1998). Although the metabolite analysis employed in this study could not discriminate between the metabolites localized in the cytosol and mitochondria, the results indicate that a sufficient supply of NADPH increases the turnover of the XR reaction and results in increased xylose uptake by YPH499XU/MAE1 (Fig. 2a). The reduced malate levels also indicate that the malate supply in the transformant was insufficient (Fig. 2d). On the other hand, the NADH/NAD^+ ratio was decreased in the YPH499XU/MAE1 strain suggesting that malate would be continuously supplied by the innate activities of PYC and MDH (Fig. 2e). The relieved intracellular redox state would activate the XDH reaction and reduced xylitol production. It is noteworthy that MAE and XR are localized in the mitochondria and cytosol, respectively (Amore et al. 1991; Boles et al. 1998). Thus, the NADPH regenerated in the mitochondria is likely to be transported to the cytosol via the mitochondrial redox shuttle (Fig. 1). A redox shuttle responsible for the transport of NADPH has not yet been identified; however, its existence has been suggested by the improved xylose fermentation observed in the recombinant strains overexpressing Mae1p (Table 2).

In order to increase the malate supply, the *PYC2* gene was additionally introduced to generate the YPH499XU/MAE1–PYC2 strain. The overexpression of Pyc2p caused a serious reduction in the specific xylose consumption rate and ethanol yield (Table 2). This result suggested that the simultaneous overexpression of Pyc2p and Mae1p under the control of the *PGK1* promoter could worsen the redox imbalance. Indeed, comparison of the carbon balance revealed that although 70.3 % of the total assimilated carbon was secreted as ethanol, xylitol, and glycerol in the case of the YPH499XU/MAE1 strain (determined from the ethanol, xylitol, and glycerol yields in Table 2), the carbon yield in YPH499XU/MAE1–PYC2 deceased to 59.6 %. These results indicate that an unknown by-product was secreted in the fermentation medium by a metabolic effect caused by the activation of the PYC reaction.

The YPH499XU/MAE1–MDH2 strain exhibited higher rates of xylose consumption and ethanol production than the YPH499XU/MAE1 strain (Fig. 3a,b and Table 2). On the other hand, the ethanol yield of the YPH499XU/MAE1 strain could not be improved by the additional expression of Mdh2p (Fig. 3b and Table 2). Intracellular metabolite analyses revealed that the NADH/NAD^+ ratio in the transformants was slightly higher than that of the vector control until 12 h after the fermentation start (Fig. 3f). The trend was clearly observed in the YPH499XU/MAE1–MDH2–PYC2 strain in which a higher NADH/NAD^+ ratio was

observed throughout the experiment (Fig. 4f). This result indicates that the transhydrogenase-like shunt could not convert all the excess NADH to NAD^+. The high NADH/NAD^+ ratio would affect the activity of XDH, resulting in the secretion of excess xylitol into the medium by this strain.

In the YPH499XU/MAE1–MDH2–PYC2 strain, the NADPH/$NADP^+$ ratio was also higher than that of the vector control (Fig. 4e). Although the metabolic state explains the faster xylose uptake observed in this strain (Fig. 4a), the result also suggests that the oxidative pentose phosphate pathway should be activated to regenerate NADPH from $NADP^+$. Since the production of xylitol via the reduction of xylose to xylitol requires the consumption of NADPH, it has been demonstrated that the production of xylitol depends on the generation of NADPH by the oxidative pentose phosphate pathway (Jeppsson et al. 2003; Verho et al. 2003) (Fig. 1) These results indicate that additional modifications in this pathway are required to improve the efficiency of xylose fermentation (Jeppsson et al. 2002).

In this study, we demonstrated that the redox state in *S. cerevisiae* during xylose fermentation can be controlled by the up-regulation of Mae1p, Mdh2p, and Pyc2p expression. A similar redox imbalance will occur in metabolically engineered yeasts because the activation of metabolic pathways to synthesize target compounds often demands NADPH, whereas suppression of ethanol production inevitably induces a surplus of NADH (Matsuda et al. 2011). The transhydrogenase-like shunt will be a useful tool to compensate for the redox imbalance associated with the engineering of yeast metabolism.

Acknowledgements This work was financed by the Industrial Technology Research Grant Program in 2011 of the New Energy and Industrial Technology Development Organization (NEDO), Japan, and Special Coordination Funds for Promoting Science and Technology, Creation of Innovation Centers for Advanced Interdisciplinary Research Areas (Innovative Bioproduction Kobe), MEXT, Japan.

Conflict of interests The authors declare that they have no competing interests.

References

Amore R, Kotter P, Kuster C, Ciriacy M, Hollenberg CP (1991) Cloning and expression in *Saccharomyces cerevisiae* of the NAD(P)H-dependent xylose reductase-encoding gene (*XYL1*) from the xylose-assimilating yeast *Pichia stipitis*. Gene 109:89–97

Anderlund M, Nissen TL, Nielsen J, Villadsen J, Rydstrom J, Hahn-Hagerdal B, Kielland-Brandt MC (1999) Expression of the *Escherichia coli pntA* and *pntB* genes, encoding nicotinamide nucleotide transhydrogenase, in *Saccharomyces cerevisiae* and its effect on product formation during anaerobic glucose fermentation. Appl Environ Microbiol 65:2333–2340

Arkblad EL, Betsholtz C, Rydstrom J (1996) The cDNA sequence of proton-pumping nicotinamide nucleotide transhydrogenase from man and mouse. Biochim Biophys Acta 1273:203–205

Bakker BM, Overkamp KM, van Maris AJ, Kotter P, Luttik MA, van Dijken JP, Pronk JT (2001) Stoichiometry and compartmentation of NADH metabolism in *Saccharomyces cerevisiae*. FEMS Microbiol Rev 25:15–37

Blombach B, Riester T, Wieschalka S, Ziert C, Youn JW, Wendisch VF, Eikmanns BJ (2011) *Corynebacterium glutamicum* tailored for efficient isobutanol production. Appl Environ Microbiol 77:3300–3310

Boles E, de Jong-Gubbels P, Pronk JT (1998) Identification and characterization of *MAE1*, the *Saccharomyces cerevisiae* structural gene encoding mitochondrial malic enzyme. J Bacteriol 180:2875–2882

Brachmann CB, Davies A, Cost GJ, Caputo E, Li J, Hieter P, Boeke JD (1998) Designer deletion strains derived from *Saccharomyces cerevisiae* S288C: a useful set of strains and plasmids for PCR-mediated gene disruption and other applications. Yeast 14:115–132

Bro C, Regenberg B, Forster J, Nielsen J (2006) *In silico* aided metabolic engineering of *Saccharomyces cerevisiae* for improved bioethanol production. Metab Eng 8:102–111

Bruinenberg PM, de Bot PHM, van Dijken JP, Scheffers WA (1983) The role of redox balances in the anaerobic fermentation of xylose by yeasts. Eur J Appl Microbiol Biotechnol 18:287–292

Eliasson A, Christensson C, Wahlbom CF, Hahn-Hagerdal B (2000) Anaerobic xylose fermentation by recombinant *Saccharomyces cerevisiae* carrying *XYL1, XYL2,* and *XKS1* in mineral medium chemostat cultures. Appl Environ Microbiol 66:3381–3386

Grotkjaer T, Christakopoulos P, Nielsen J, Olsson L (2005) Comparative metabolic network analysis of two xylose fermenting recombinant *Saccharomyces cerevisiae* strains. Metab Eng 7:437–444

Hahn-Hagerdal B, Karhumaa K, Jeppsson M, Gorwa-Grauslund MF (2007) Metabolic engineering for pentose utilization in *Saccharomyces cerevisiae*. Adv Biochem Eng Biotechnol 108:147–177

Hasunuma T, Sung KM, Sanda T, Yoshimura K, Matsuda F, Kondo A (2011) Efficient fermentation of xylose to ethanol at high formic acid concentrations by metabolically engineered *Saccharomyces cerevisiae*. Appl Microbiol Biotechnol 90:997–1004

Ho NW, Chen Z, Brainard AP (1998) Genetically engineered *Saccharomyces* yeast capable of effective cofermentation of glucose and xylose. Appl Environ Microbiol 64:1852–1859

Hsiao H-Y, Chiang L-C, Ueng PP, Tsao GT (1982) Sequential utilization of mixed monosaccharides by yeasts. Appl Environ Microbiol 43:840–845

Ishii J, Izawa K, Matsumura S, Wakamura K, Tanino T, Tanaka T, Ogino C, Fukuda H, Kondo A (2009) A simple and immediate method for simultaneously evaluating expression level and plasmid maintenance in yeast. J Biochem 145:701–708

Ito H, Fukuda Y, Murata K, Kimura A (1983) Transformation of intact yeast cells treated with alkali cations. J Bacteriol 153:163–168

Jeffries TW, Jin YS (2004) Metabolic engineering for improved fermentation of pentoses by yeasts. Appl Microbiol Biotechnol 63:495–509

Jeppsson M, Johansson B, Hahn-Hagerdal B, Gorwa-Grauslund MF (2002) Reduced oxidative pentose phosphate pathway flux in recombinant xylose-utilizing *Saccharomyces cerevisiae* strains improves the ethanol yield from xylose. Appl Environ Microbiol 68:1604–1609

Jeppsson M, Johansson B, Jensen PR, Hahn-Hagerdal B, Gorwa-Grauslund MF (2003) The level of glucose-6-phosphate dehydrogenase activity strongly influences xylose fermentation and inhibitor sensitivity in recombinant *Saccharomyces cerevisiae* strains. Yeast 20:1263–1272

Johansson B, Hahn-Hagerdal B (2002) The non-oxidative pentose phosphate pathway controls the fermentation rate of xylulose

but not of xylose in *Saccharomyces cerevisiae* TMB3001. FEMS Yeast Res 2:277–282

Kötter P, Ciriacy M (1993) Xylose fermentation by *Saccharomyces cerevisiae*. Appl Microbiol Biotechnol 38:776–783

Katahira S, Ito M, Takema H, Fujita Y, Tanino T, Tanaka T, Fukuda H, Kondo A (2008) Improvement of ethanol productivity during xylose and glucose co-fermentation by xylose-assimilating *S. cerevisiae* via expression of glucose transporter Sut1. Enzyme Microb Technol 43:115–119

Katahira S, Mizuike A, Fukuda H, Kondo A (2006) Ethanol fermentation from lignocellulosic hydrolysate by a recombinant xylose- and cellooligosaccharide-assimilating yeast strain. Appl Microbiol Biotechnol 72:1136–1143

Kato H, Izumi Y, Hasunuma T, Matsuda F, Kondo A (2012) Widely targeted metabolic profiling analysis of yeast central metabolites. J Biosci Bioeng 113:665–673

Klimacek M, Krahulec S, Sauer U, Nidetzky B (2010) Limitations in xylose-fermenting *Saccharomyces cerevisiae*, made evident through comprehensive metabolite profiling and thermodynamic analysis. Appl Environ Microbiol 76:7566–7574

Krahulec S, Petschacher B, Wallner M, Longus K, Klimacek M, Nidetzky B (2010) Fermentation of mixed glucose–xylose substrates by engineered strains of *Saccharomyces cerevisiae*: role of the coenzyme specificity of xylose reductase, and effect of glucose on xylose utilization. Microb Cell Fact 9:16

Matsuda F, Furusawa C, Kondo T, Ishii J, Shimizu H, Kondo A (2011) Engineering strategy of yeast metabolism for higher alcohol production. Microb Cell Fact 10:70

Matsushika A, Inoue H, Kodaki T, Sawayama S (2009) Ethanol production from xylose in engineered *Saccharomyces cerevisiae* strains: current state and perspectives. Appl Microbiol Biotechnol 84:37–53

Matsushika A, Watanabe S, Kodaki T, Makino K, Sawayama S (2008) Bioethanol production from xylose by recombinant *Saccharomyces cerevisiae* expressing xylose reductase, NADP(+)-dependent xylitol dehydrogenase, and xylulokinase. J Biosci Bioeng 105:296–299

Moreira dos Santos M, Raghevendran V, Kotter P, Olsson L, Nielsen J (2004) Manipulation of malic enzyme in *Saccharomyces cerevisiae* for increasing NADPH production capacity aerobically in different cellular compartments. Metab Eng 6:352–363

Nevoigt E (2008) Progress in metabolic engineering of *Saccharomyces cerevisiae*. Microbiol Mol Biol Rev 72:379–412

Nissen TL, Anderlund M, Nielsen J, Villadsen J, Kielland-Brandt MC (2001) Expression of a cytoplasmic transhydrogenase in *Saccharomyces cerevisiae* results in formation of 2-oxoglutarate due to depletion of the NADPH pool. Yeast 18:19–32

Pitkanen JP, Aristidou A, Salusjarvi L, Ruohonen L, Penttila M (2003) Metabolic flux analysis of xylose metabolism in recombinant *Saccharomyces cerevisiae* using continuous culture. Metab Eng 5:16–31

Rizzi M, Erlemann P, Bui-Thanh N, Dellweg H (1988) Xylose fermentation by yeasts: 4. Purification and kinetic studies of xylose reductase from Pichia stipitis. Appl Microbiol Biotechnol 29:148–154

Rizzi M, Harwart K, Erlemann P, Bui-Thanh N, Dellweg H (1989) Purification and properties of the NAD+-xylitol-dehydrogenase from the yeast *Pichia stipitis*. J Ferment Bioeng 67:20–24

Sauer U, Canonaco F, Heri S, Perrenoud A, Fischer E (2004) The soluble and membrane-bound transhydrogenases UdhA and PntAB have divergent functions in NADPH metabolism of *Escherichia coli*. J Biol Chem 279:6613–6619

Sonderegger M, Jeppsson M, Hahn-Hagerdal B, Sauer U (2004) Molecular basis for anaerobic growth of *Saccharomyces cerevisiae* on xylose, investigated by global gene expression and metabolic flux analysis. Appl Environ Microbiol 70:2307–2317

Sonderegger M, Sauer U (2003) Evolutionary engineering of *Saccharomyces cerevisiae* for anaerobic growth on xylose. Appl Environ Microbiol 69:1990–1998

Spura J, Reimer LC, Wieloch P, Schreiber K, Buchinger S, Schomburg D (2009) A method for enzyme quenching in microbial metabolome analysis successfully applied to gram-positive and gram-negative bacteria and yeast. Anal Biochem 394:192–201

Tantirungkij M, Nakashima N, Seki T, Yoshida T (1993) Construction of xylose-assimilating *Saccharomyces cerevisiae*. J Ferment Bioeng :83–88

Van Vleet JH, Jeffries TW (2009) Yeast metabolic engineering for hemicellulosic ethanol production. Curr Opin Biotechnol 20:300–306

Verho R, Londesborough J, Penttila M, Richard P (2003) Engineering redox cofactor regeneration for improved pentose fermentation in *Saccharomyces cerevisiae*. Appl Environ Microbiol 69:5892–5897

Watanabe S, Abu Saleh A, Pack SP, Annaluru N, Kodaki T, Makino K (2007) Ethanol production from xylose by recombinant *Saccharomyces cerevisiae* expressing protein-engineered NADH-preferring xylose reductase from *Pichia stipitis*. Microbiology 153:3044–3054